JOURNAL OF AEROSOL MEDICINE
Volume 20, Number 1, 2007

Pp. 59–74
DOI: 10.1089/jam.2006.0531

Characterization of Deposition from Nasal Spray Devices Using a Computational Fluid Dynamics Model of the Human Nasal Passages

JULIA S. KIMBELL, Ph.D.,[1] REBECCA A. SEGAL, Ph.D.,[1] BAHMAN ASGHARIAN, Ph.D.,[1] BRIAN A. WONG, Ph.D.,[1] JEFFRY D. SCHROETER, Ph.D.,[1] JEREMY P. SOUTHALL, Ph.D.,[2] COLIN J. DICKENS,[2] GEOFF BRACE,[2] and FREDERICK J. MILLER, Ph.D.[1]

ABSTRACT

Many studies suggest limited effectiveness of spray devices for nasal drug delivery due primarily to high deposition and clearance at the front of the nose. Here, nasal spray behavior was studied using experimental measurements and a computational fluid dynamics model of the human nasal passages constructed from magnetic resonance imaging scans of a healthy adult male. Eighteen commercially available nasal sprays were analyzed for spray characteristics using laser diffraction, high-speed video, and high-speed spark photography. Steady-state, inspiratory airflow (15 L/min) and particle transport were simulated under measured spray conditions. Simulated deposition efficiency and spray behavior were consistent with previous experimental studies, two of which used nasal replica molds based on this nasal geometry. Deposition fractions (numbers of deposited particles divided by the number released) of 20- and 50-μm particles exceeded 90% in the anterior part of the nose for most simulated conditions. Predicted particle penetration past the nasal valve improved when (1) the smaller of two particle sizes or the lower of two spray velocities was used, (2) the simulated nozzle was positioned 1.0 rather than 0.5 or 1.5 cm into the nostril, and (3) inspiratory airflow was present rather than absent. Simulations also predicted that delaying the appearance of normal inspiratory airflow more than 1 sec after the release of particles produced results equivalent to cases in which no inspiratory airflow was present. These predictions contribute to more effective design of drug delivery devices through a better understanding of the effects of nasal airflow and spray characteristics on particle transport in the nose.

Key words: computational fluid dynamics, particle desposition, nasal spray, nasal value, spray characteristics

INTRODUCTION

THE ADMINISTRATION of inhaled therapeutics via the nasal mucosa can lead to enhanced drug delivery both locally and systemically.(1) Advantages of nasal drug delivery include a large surface area for absorption,(2) relatively rapid delivery to systemic circulation, and avoidance of the gastrointestinal tract with first-pass metabolism in the liver.(3) Intranasal delivery is noninvasive

[1]The Hamner Institutes for Health Sciences.
[2]Bespak Europe Ltd., Milton Keynes, United Kingdom.

and is considered a potential replacement delivery method for some medications currently requiring injection.[1,4] This substitution should improve patient compliance with prescription instructions and is especially attractive for children. In addition, the spectrum of potential therapeutic areas is large, ranging from crisis management and vaccination to treatments for many disease states involving the respiratory tract and other organ systems.[3]

The delivery of drugs via the nasal passages also faces some challenges. Experimental studies indicate that many nasal spray devices deposit most of their material in the anterior portion of the nose,[2,5–10] with little of the spray reaching the turbinates.[5] To be efficacious, nasally delivered drugs must have a high potency, potentially leading to side effects including nasal tissue irritation[3] and taste aversion. Optimal intranasal distribution of nasal sprays usually requires that the delivered spray penetrate the nasal valve area.[11] In addition, the drug must survive mucociliary clearance and pass through the enzyme-rich nasal mucosa to reach systemic circulation.[3] Therefore, nasal drug delivery will be improved by efforts to understand both delivery and formulation issues.

Quantitative data on device performance are available that allow some comparisons to be made among different delivery methods, spray angles, particle sizes, and patient-related factors such as inhaler orientation, head position, and inspiratory airflow rates (Table 1). These studies imply that nasal sprays result in fairly targeted deposition patterns[2,5] that cover more area, are retained longer, and may penetrate the nose better if spray velocity, spray angle, and particle size are decreased.[2,7,12] The studies also imply that inhaler and patient positioning and the speed of inspiratory airflow do not have much effect on the regional deposition of nasal sprays.[6,8,10,13,14] However, no comprehensive study of the sensitivity of nasal deposition patterns to a series of different spray characteristics, particularly particle size, under normal use conditions is available, in part because such a study is complex and the associated experiments are expensive. Yet this information could provide a better understanding of the interactions between nasal anatomy, sprays, and spray devices that could be used to improve nasal drug delivery.

The main obstruction to adequate delivery of nasal sprays is the nasal valve,[15] the region of maximum resistance to airflow located in the anterior part of the nose.[16] The nasal valve is described in several different ways in the medical literature. It is formed by the cartilaginous tissues of the external area of the nose, the pyriform aperture of the skull, and some medical descriptions include the anterior aspects of the middle and inferior turbinates.[17,18] Other sources define the nasal valve in conjunction with acoustic rhinometry as the part of the nose in which the cross-sectional area of the nasal airways is minimized.[16,19] Nasal sprays intended to reach the ciliated mucosa of the nose must penetrate the

Table 1. Experimental Studies Comparing Methods of Nasal Drug Delivery

Delivery method	*Experimental findings*		
Metered aerosol vs. metered spray pump	No differences in regional deposition[6]		
Drops vs. spray	Drops coated more nasal surface and cleared faster[5]	Variable delivery to middle meatus[11]	
Nebulizer vs. spray pump	Nasal nebulizer enhanced posterior and superior nasal deposition[2]		
Effect of spray angle	Decreased angle lowered particle retention and increased deposition area[7]	Increased angle increased anterior nose deposition[12]	
Effect of particle size	Increased size increased anterior nose deposition[12]		
Inhaler orientation	No effects on quantity reaching nose or initial distribution pattern[8]		
Head position	No effect on spray distribution[10]		
Effect of inspiratory airflow	No effect on regional deposition[6]	No effect on distribution patterns[13]	No effect on distribution patterns[14]

nasal valve region. More information on the roles different spray characteristics play in enhancing the penetration of the spray past the nasal valve is needed in order to improve nasal drug delivery.

An alternative approach to studying the role of spray devices and characteristics in nasal valve penetration is to use three-dimensional computer modeling. Anatomically accurate, three-dimensional computer models of the human nasal passages have been constructed from sectioned casts,[20,21] computed tomography (CT) scans,[22–25] and magnetic resonance imaging (MRI) scans.[26] Computational fluid dynamics (CFD) methods have been used to simulate airflow[20–23,26] as well as particle transport[20,23] in the lumen of the human nose.

In the present study, nasal spray behavior was studied using the CFD model of Subramaniam and colleagues,[26] in-house particle transport software,[27] and experimental studies characterizing the sprays from 18 different commercially available nasal spray devices.[28] The nasal valve region of the CFD model was identified to allow calculation of the fraction of sprayed material that was predicted to penetrate past this area. Experimentally, spray angles ranged in size from 32° to 79°, average spray velocities ranged from 1.5 to 14.7 m/sec, and droplet sizes averaged about 50 μm.[28] This information was used as the basis for estimating the effects of three nozzle positions, two spray angles, two spray velocities, two particle sizes, and the presence, delayed presence, or absence of inspiratory airflow on the fraction of sprayed material that penetrated the nasal valve. The main purposes of this study were to (1) confirm that the CFD model could capture particle and spray behavior as described in previous experimental studies, (2) suggest reasons for limitations evident in current drug delivery via nasal sprays, and (3) suggest potential ways in which spray penetration could be improved.

MATERIALS AND METHODS

In this section, overviews of the CFD and particle transport models are given with descriptions of the major assumptions upon which the models and simulations are based. The simulation of spray releases and estimated nozzle positions in the nasal vestibule are described. The nasal valve area of the model is defined and used to estimate the fraction of particles that were predicted to deposit in the nose posterior to this location. The predicted effects of multiple combinations of spray characteristics on nasal valve penetration are described by conducting a series of spray simulations under conditions described below. Comparisons of total nasal deposition efficiency and spray behavior predicted using the CFD model with experimental measurements are made.

Simulation of nasal airflow and particle transport

A three-dimensional, human nasal CFD model provided the anatomical shape, computational mesh, and inspiratory airflow patterns used in the simulations conducted here. This CFD model and a comparison of simulated airflow with experimental measurements were described in detail by Subramaniam and colleagues.[26] Briefly, a finite-element mesh (Fig. 1A)[29] was constructed from 72 cross sections, spaced 1.5 mm apart, based on MRI scans of a healthy, adult, nonsmoking male using in-house software[30] and the commercial CFD package FIDAP (Fluent, Inc., Lebanon, NH). The mesh was constructed of six-sided, brick-shaped elements and contained approximately 156,000 nodes. FIDAP was also used to simulate steady-state airflow in the inspiratory direction at 15 L/min with a uniform velocity profile (plug flow) imposed at the nostrils, velocity set to zero at airway walls (no-slip condition), and the normal velocity gradients set to zero at the outlet. Simulated airflow velocities within the nose were confirmed using published measurements.[26]

The major patterns of inhaled airflow simulated at steady-state were assumed to be similar to those occurring during resting breathing based on calculation of the Strouhal number, or frequency parameter.[26] Unsteady effects may be considered insignificant when the frequency parameter is less than 1.[31] The Strouhal number, $S = \omega L/u$, where ω, L, and u are the breathing frequency, axial length of the nasal airway, and the average velocity, respectively, is 0.02 in the human, using $\omega = 0.25$ Hz, L = 11 cm, and u = 144 cm/sec, corresponding to a flow rate of 26 L/min and a cross-sectional area of 3 cm^2.[26] The CFD model had rigid nasal walls, lacked mucus movement and nasal hairs, and did not account for gain or loss of heat or humidity. These modeling constraints were assumed to contribute insignificantly to error in airflow simulations.

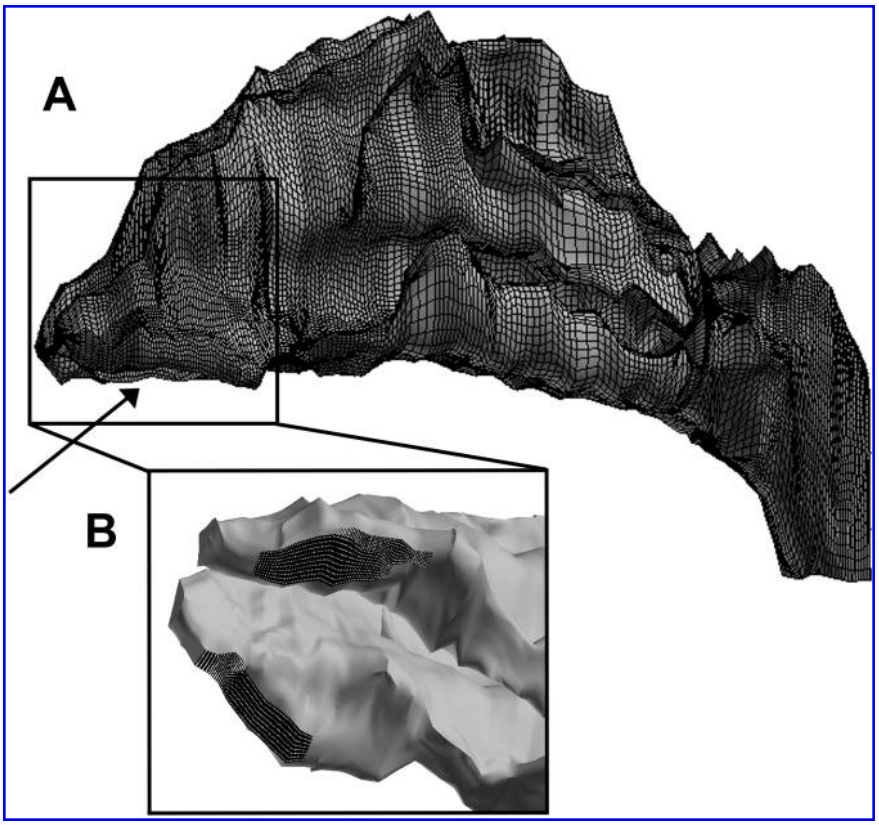

FIG. 1. (**A**) Lateral view of the finite-element mesh used in the computational fluid dynamics simulations. Nostrils are to the left at arrow, nasopharynx is to the right. Reprinted with permission from Ref. (29). (**B**) Ventral view of nostrils (black) showing locations of passive particle release points (white dots) for prediction of nasal deposition efficiency.

Because particles measured in many nasal spray products largely exceeded 5 μm in diameter, sedimentation, and inertial impaction are likely to be the prevailing particle deposition mechanisms. Thus, the equations of motion for particle transport were solved numerically for the case when inertial forces are dominant. Particle-to-particle and particle-to-flow interactions were assumed to be negligible, allowing airflow and particle transport equations to decouple. These interactions would become increasingly significant if particle volume density in the breathing air approached unity or if particle inertia became large enough to affect surrounding airflow patterns, conditions that did not apply to the simulations presented here.

Airflow information was obtained from the FIDAP simulations described above. Single-particle trajectories were calculated using the airflow information as input to software developed in-house that solved the Lagrangian form of the equations of particle transport numerically.[27] A computer algorithm, developed in C++ and implemented in Java, calculated particle trajectory using a Runge-Kutta scheme with variable time steps. The error in numerical simulations was calculated at every particle location and checked against a predetermined tolerance. The time step was then either reduced to improve the accuracy of the simulations or increased to shorten runtime. Particle trajectories were calculated until the particle deposited, exited the nasal airway passages, or the travel time exceeded a predetermined time scale typically near the breathing time or a multiple thereof (e.g., 4 sec based on 15 breaths per minute). The in-house particle solver used to track particle movement has been validated and used in other studies involving aerosol transport.[32]

Simulation of nasal sprays

Particle trajectory calculations allowed the initial velocity of particles to be non-zero to simu-

late launching via a spray device. Particle trajectories from simulated spray releases were calculated both in the presence, at 15 L/min, and in the absence of inspiratory nasal airflow. When airflow was present, no spray device was depicted as present in the nasal vestibule and it was assumed that there was no disruption of normal inspiratory airflow patterns while particles were being transported. To account for time between spray activation and inspiration, trajectory calculations included the option to begin trajectory calculation with no airflow present and introduce normal inspiratory airflow vectors at a later time point.

For each point of release, a group of particles representing a spray cone was instantaneously discharged with a specified spray cone angle and spray velocity. The group of spray particles consisted of a center particle launched from a release point with up to three concentric rings of eight particles each (subsprays) launched around the center particle from the same release point. The initial direction of the center particle's motion was determined by the ray from a fixed nostril reference point to the particle release point (Fig. 2). The initial directions of the subspray particles' motion were determined by evenly spaced rays at angular intervals from 0° to the spray cone angle. The spacing of the subsprays was such that all sphere sectors formed by initial spray vector tips were of equal area. The duration or lifetime of the spray, potential effects of sprays on normal inspiratory airflow patterns, and interactions of spray particles with each other were not simulated.

Three sets of particle release points, located 0.5, 1.0, and 1.5 cm into the left nostril, represented possible nozzle tip locations. Comfortable use limited the angle at which the spray nozzle was tilted to between 55° and 75° from the horizontal in the sagittal plane (Fig. 2). Each set of release points consisted of a curved surface of evenly spaced lattice of points lying between 55° and 75° from the horizontal plane inside the nasal vestibule, equidistant from a single reference point located on the nostril surface (Fig. 3).

All release points at a given nozzle penetration depth were considered equally representative of potential spray release locations because of variability in patient use of spray devices. Results from spray releases at all lattice points on a given release surface were therefore aggregated to re-

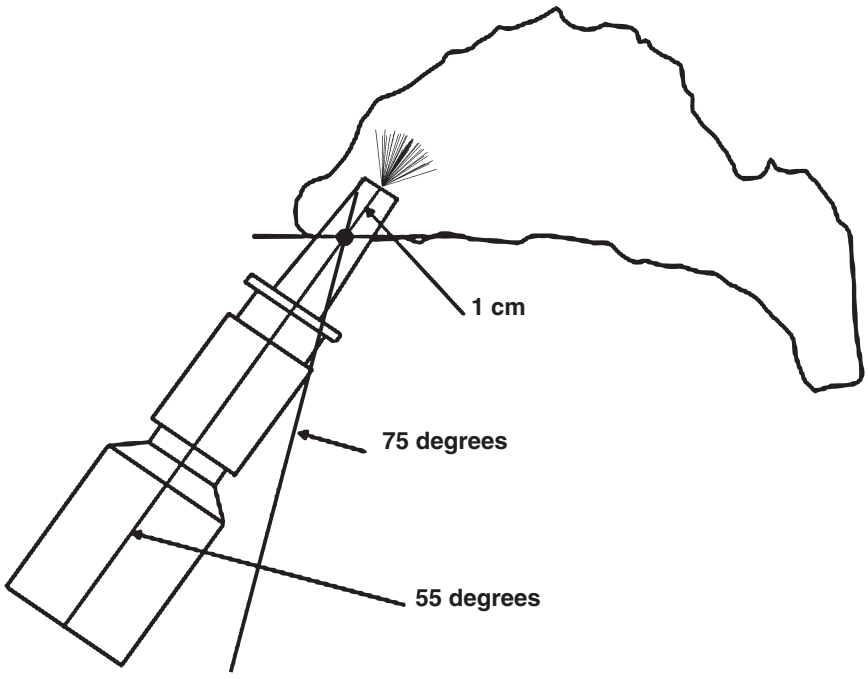

FIG. 2. Side view of nasal model and inserted nasal spray device showing a simulated spray originating from a release point in relation to the nostril reference point (black dot), and the range of comfortable nozzle positions from 55° from the horizontal to 75° when the spray device is inserted 1 cm into nostril. Nostril reference point (black dot) represents the intersection of the axis of the device with the nostril surface.

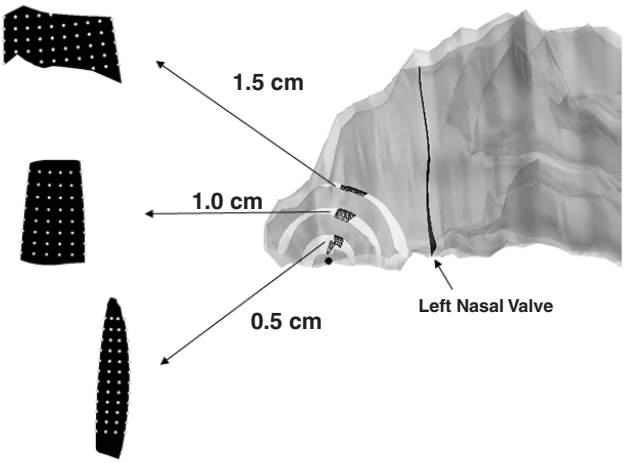

FIG. 3. Locations of potential spray release points and left nasal valve. White spherical pieces indicate all points in left side of the nose that are located 0.5, 1.0, and 1.5 cm from the nostril reference point (black dot). Areas of potential spray release (black patches on white spherical pieces) appear as subsets of the white spherical pieces when the nozzle tip was allowed to vary between 55° and 75° from the horizontal. Closeups show the most coarse lattice of spray release points (gray dots) used in the simulations.

duce effects of this variability on nasal valve penetration.

The nasal valve

A planar section in the anterior portion of the CFD model with minimum coronal cross-sectional area was found by first sweeping a plane perpendicular to the axial direction (90° from the horizontal in the sagittal plane) through the model and sampling cross-sectional area.[33] This plane was then tilted away from the top of the head at 1° increments from 90° to 6° from the horizontal in the sagittal plane and cross-sectional area was sampled by sweeping each tilted plane through the CFD model. Planes tilted from 90° to 65° were also tilted by 1° increments from 0° to 25° in the axial plane and swept through the model to obtain cross-sectional area samples. Minimum cross-sectional area was obtained separately for each side of the nose (Fig. 3).

To confirm model predictions of minimum cross-sectional area for identification of the nasal valve area, comparisons were also needed with laboratory and clinical measurements. These comparisons can be difficult to interpret because human nasal anatomy differs significantly among individuals. Therefore, two copies of hollow, plastic molds of the nasal passages were created from the same geometry that underlies the CFD model using a computer-aided design/computer-aided manufacturing (CAD/CAM) technique called stereolithography.[34–36] Acoustic rhinometry (Acoustic Rhinometer, Hood Laboratories, Pembroke, MA) was then used to measure cross-sectional area in both sides of the nasal passage in both plastic molds for comparison with the minimum cross-sectional area calculated in the CFD model and with values reported in the literature.

Predictions of nasal spray behavior

Particle transport simulations were based on analyses of 18 nasal sprays for particle size distribution and spray characteristics.[28] Particle transport in the left-hand side of the nose under measured spray conditions was simulated, and effects of three nozzle positions, two particle sizes, two spray angles, two spray velocities, and the presence, delayed presence, or absence of inspiratory airflow on particle penetration past the nasal valve area were calculated. Southall and colleagues[28] measured particle size distributions and found that most particles were between 50 and 70 μm (mass median aerodynamic diameter), with sizes ranging from 20 to 150 μm. Simulations were conducted for 20- and 50-μm particles released from nozzle penetration distances of 0.5, 1.0, and 1.5 cm. These particle sizes were chosen to better understand published studies (Table 1; 50 μm) as well as to extend this understanding in an attempt to improve nasal valve penetration (20 μm). Spray cone angles of 32° and 79° were used, representing the extremes of the range of measured angles. Spray velocities were set to 1 and 10 m/sec, representative of sprays in the measured range from 1.5 to 14.7 m/sec. Simulations also included either the presence or absence of nasal inspiratory airflow at 15 L/min, resulting in a total of 48 simulation cases. In addition, the effect of time delays of 0.5 and 1.0 sec between the release of particles and the presence of inspiratory airflow was studied for several cases. Simulations were also conducted in which 20- and 50-μm particles were passively released from the left nostril inlet surface (Fig. 1B) with steady-state, inspiratory airflow present at 15 L/min for comparison with spray simulations. The effect of 30 L/min inspiratory airflow on left nasal valve penetration of 20- and 50-μm particles released

from 1 cm into the nostril with a 1 m/sec, 79° spray was also studied in an attempt to identify conditions that improved nasal valve penetration.

The influence of the density of release points and the density of particles released in each spray cone on these results were examined for the case where nozzle penetration distance was set to 1 cm. Three release point densities were used: a base mesh (6 points × 8 points), a refined mesh (9 points × 12 points), and a fine mesh (12 points × 16 points). Three spray densities were used: a coarse spray (center particle and one subspray released at the spray angle), a refined spray (center particle and two subsprays), and a fine spray (center particle and three subsprays).

The deposition fractions reported here were calculated as aggregates over all release points on a surface representing most potentially comfortable nozzle positions. In a study using a physical model based on the same nasal geometry as the CFD model used here, Cheng and colleagues[12] studied spray deposition patterns that were the result of sprays released from one (unspecified) nozzle position. In order to compare simulated results with the Cheng study,[12] nasal valve penetration predicted for the best 20- and 50-μm simulation cases was also examined for each individual release point.

Confirmation of particle deposition predictions

To confirm CFD model predictions, comparisons of simulation results with two types of experimental studies were made: measurements of nasal spray deposition and measurements of nasal deposition efficiency. Results from the simulation of nasal spray behavior as described above for 20- and 50-μm particles were compared with the results reported by the studies cited in Table 1. Because nasal deposition efficiency is approximately 100% for particles 20 μm or greater that are inhaled at 15 L/min,[37] comparisons of predicted deposition efficiency with experimental studies were made for particle sizes less than 20 μm.

Most of the experiments that have been conducted to measure nasal deposition efficiency *in vivo* have produced estimates from inhalation of particle-laden atmospheres.[38–44] In two of these studies, air was drawn in through the nose from the mouth at several flow rates while the subject held their breath.[38,40] Measurements of the deposition of either 1- to 9-μm methylene blue solution aerosols[38] or radioactive polystyrene particles, approximately 2 to 8 μm in aerodynamic diameter,[40] were made using filters.

Nasal deposition efficiency was also measured in copies of the hollow plastic replica molds used for acoustic rhinometry, as described in the Nasal Valve section above.[36] In these experiments, liquid droplets between 1 and 10 μm in aerodynamic diameter were drawn through the hollow mold at several flow rates. Particle concentrations were measured at the inlet and outlet of the nasal mold and were used to calculate deposition efficiency.

The present study focused on large particle transport in which sedimentation and inertial forces are dominant. Comparisons of model predictions with experimental measurements were therefore confined to particles >5 μm in diameter. To compare model predictions with these measurements, simulations were conducted in which particles ranging from 6 to 10 μm in diameter were passively released from both nostril inlet surfaces (Fig. 1B) with steady-state, inspiratory airflow present at 20 L/min. This flow rate was selected as one used by all three of the Pattle,[38] Hounam,[40] and Kelly[36] studies that was close to the flow rate of 15 L/min used in the simulations of nasal sprays. Deposition efficiency was calculated by weighting each particle that deposited by the proportion of flow through the nostril element from which the particle originated and aggregating these results for all deposited particles.

Data analysis

Predictions of the number of particles that deposited, deposition locations, and particle trajectories were recorded. Deposition fractions, defined as the number of deposited particles divided by the number of particles released and expressed as a percentage, were calculated for the entire nasal passages and for the nasal vestibule anterior to the nasal valve plane. Of the particles predicted to deposit, those that passed the nasal valve plane were identified.

An analysis was conducted to determine whether there were statistically significant differences among nasal valve penetration fractions when individual simulation parameters were changed. The simulation data represented a completely randomized design with five factors: dis-

tance of the spray nozzle from the nostril, airflow presence or absence, particle size, spray velocity, and spray angle. Distance from the nostril had three values whereas the other factors had two each, resulting in a total of 48 factor combinations. The outcome variable was the percent of deposited particles penetrating the nasal valve. An arcsine transformation,[45] which is commonly used with percentage data, was applied to the outcome variable to ensure adherence to the assumptions needed for analysis of variance (ANOVA). Given the large number of factor combinations of interest (48 cases), ANOVA methods were preferable to less powerful nonparametric methods. The ANOVA included all five main effects and all 10 first-order interactions.

RESULTS

Anatomical factors affecting spray deposition

Based on the geometric constraints on nozzle position used in these studies, namely, that the nozzle did not penetrate further than 1.5 cm into the nose and that nozzle tilts in the sagittal plane from 55° to 75° represented limits of a comfortable range of nozzle positions, CFD predictions indicated that spray devices release particles within very small, constricted regions in the nasal vestibule (Fig. 3). The approximate surface area of each the three release surfaces identified in this study was less than 0.20 cm^2.

The minimum cross-sectional area for the left side of the nose, defined as the position of the nasal valve for this study, was estimated to be 0.72 cm^2, located on a plane tilted 90° toward the top of the head in the sagittal plane and 7° toward the left side of the nose in the axial plane, at an average distance of about 3 cm from the nostril surface (Table 2). The minimum cross-sectional area for the right side of the nose was estimated to be 0.64 cm^2, located on a plane tilted 70° toward the top of the head in the sagittal plane and 15° toward the left side of the nose in the axial plane, at an average distance from the nostril on the left side of about 3 cm. Minimum cross-sectional area for the left side as measured by acoustic rhinometry was 0.65 cm^2 in one stereolithography mold and 0.68 cm^2 in the other, at an approximate distance of 2.3 cm from the nostril. Minimum cross-sectional area for the right side as measured by acoustic rhinometry was 0.64 cm^2 in one stereolithography mold and 0.66 cm^2 in the other, at an approximate distance of 2.3 cm from the nostril. The plane where cross-sectional area on the left side of the nose was minimized was used to define the nasal valve for the purposes of the studies described here.

Predictions of nasal spray behavior

In all simulated cases described in this paper, no particles were predicted to pass entirely through the nasal passages, i.e., all spray deposition fractions of 20- and 50-μm particles were 100% in the nasal passages, except in three cases in which some of the released particles were predicted to fall out of the nose through the nostril because of sedimentation (Table 3). Out of 48 spray simulation cases, 15 resulted in a non-zero percentage of particles predicted to penetrate the left nasal valve (Table 3). Deposition fractions in the nasal vestibule exceeded 90% under most simulated conditions. Most particles that penetrated the nasal valve were predicted to deposit on the middle and inferior turbinates and the adjacent lateral walls and septum. Simulations predicted that spray deposition patterns were generally dorsal when the spray nozzle was placed 1.5 cm into the nostril and showed ventral deposition when the nozzle was placed at 0.5 cm into the nostril (Fig. 4).

Table 2. Minimum Cross-Sectional Area in a CFD Model and Plastic Molds of the CFD Model

	Left side		*Right side*	
Model	*Area (cm^2)*	*Distance from nostril (cm)*	*Area (cm^2)*	*Distance from nostril (cm)*
Plastic Mold A[a]	0.65	2.3	0.64	2.3
Plastic Mold B[a]	0.68	2.3	0.66	2.3
CFD Model[b]	0.72	3	0.64	3

[a]Measured using an acoustic rhinometer.
[b]Predicted by planar cross-sectional area.

TABLE 3. PREDICTED PENETRATION OF NASAL VALVE BY PARTICLES RELEASED FROM CURRENTLY MARKETED NASAL SPRAY DEVICES (NONZERO CASES)

Distance from nostril (cm)	*Airflow rate (L/min)*	*Particle size (μm)*	*Spray velocity (m/sec)*	*Spray angle (degrees)*	*% Deposition*	*% Falling out nostril*	*% Passing left NV*
0	15	20	NA[a]	NA	100	0	9
0	15	20	NA[a]	NA	100	0	2
0.5	0	50	1	79	98	2	0[b]
0.5	0	20	1	32	55	45	0[b]
0.5	0	20	1	79	52	48	0[b]
0.5	15	50	1	32	100	0	3
0.5	15	50	1	79	100	0	2
0.5	15	20	10	32	100	0	1
0.5	15	20	10	79	100	0	2
0.5	15	20	1	32	100	0	6
0.5	15	20	1	79	100	0	6
1	15	50	10	79	100	0	1
1	15	50	1	32	100	0	4
1	15	50	1	79	100	0	4
1	15	20	10	79	100	0	1
1	15	20	1	32	100	0	18
1	15	20	1	79	100	0	19
1.5	15	50	1	79	100	0	1
1.5	15	20	1	32	100	0	3
1.5	15	20	1	79	100	0	4

[a]NA, not applicable. These studies represent simulations of particles passively released from the left nostril surface.

[b]These cases are included to show predicted loss of sprayed particles through nostril by sedimentation.

NV, nasal valve.

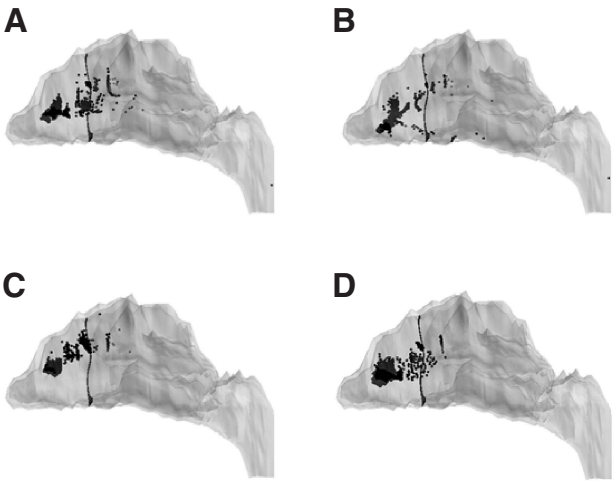

FIG. 4. Examples of deposition patterns in cases for which nasal valve penetration was high. The left nasal valve is indicated as a black cross section in all views. Steady-state, inspiratory airflow at 15 L/min was present, spray velocity was 1 m/sec, and spray angle was 79° in all cases shown here. (**A**) Nasal valve penetration, 19% (highest case); particle size, 20 μm; nozzle penetration distance, 1.0 cm. (**B**) Nasal valve penetration, 6%; particle size, 20 μm; nozzle penetration distance, 0.5 cm. (**C**) Nasal valve penetration, 4%; particle size, 20 μm; nozzle penetration distance, 1.5 cm. (**D**) Nasal valve penetration, 4% (highest 50–μm case); particle size, 50 μm; nozzle penetration distance, 1.0 cm.

More particles were predicted to pass the nasal valve before depositing when the spray nozzle was placed 1 cm into the nostril, airflow was present, and 20-μm particles were released with a velocity of 1 m/sec and a cone angle of either 32° or 79° than when sprays were simulated under other combinations of conditions (Fig. 4; Table 3). Simulations predicted that no more than about 20% of spray particles passed the nasal valve before depositing under the conditions of this study (Table 3).

Predictions of the fraction of particles that passed the nasal valve before depositing showed statistically significant improvement (Fig. 5) when (1) particle size and spray velocity decreased ($p < 0.001$), (2) nozzle penetration distance was equal to 1 cm ($p < 0.002$), and (3) airflow was present ($p < 0.001$). Effects of spray angle on predicted nasal valve penetration were not statistically significant, though there was generally a slight increase in the fraction penetrating the nasal valve when spray angle increased. Of all the simulation conditions studied, particle penetration past the nasal valve was most sensitive to the presence of inspiratory airflow, spray velocity, and particle size.

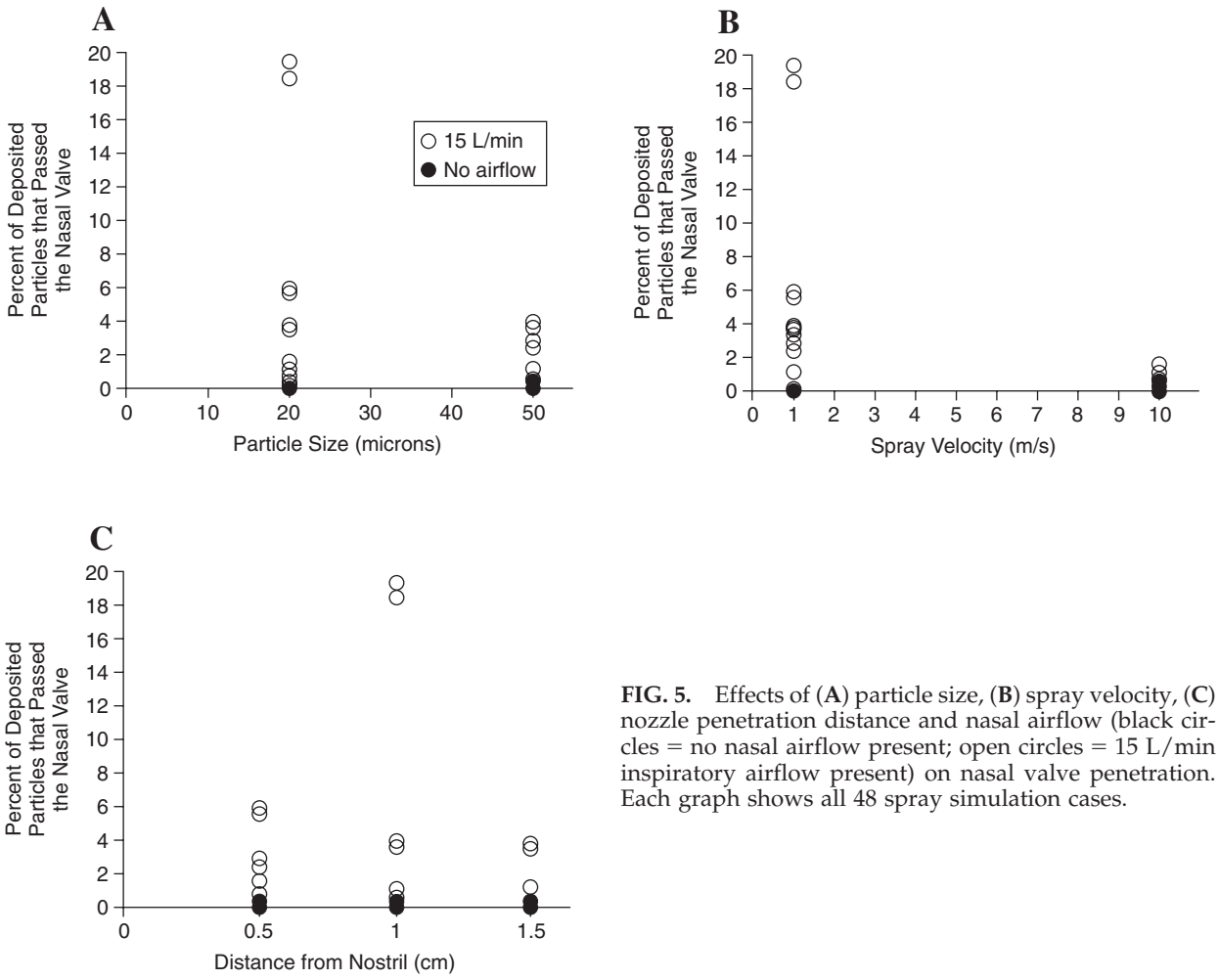

FIG. 5. Effects of (**A**) particle size, (**B**) spray velocity, (**C**) nozzle penetration distance and nasal airflow (black circles = no nasal airflow present; open circles = 15 L/min inspiratory airflow present) on nasal valve penetration. Each graph shows all 48 spray simulation cases.

The statistically significant improvements in predicted nasal valve penetration were represented graphically by grouping all 48 spray simulation cases by each of three variables: particle size (Fig. 5A), spray velocity (Fig. 5B), and nozzle position (Fig. 5C). When the 48 cases in each graph were further marked by whether inspiratory airflow was present (Fig 5, open circles) or not (Fig. 5, closed circles), the advantage of having airflow present was evident. Otherwise, each graph showed the trend for one variable at a time.

The effect of a time delay of 0.5 sec between the release of particles and the appearance of normal inspiratory airflow was studied for the cases in which the number of particles predicted to pass the nasal valve before depositing was highest. The simulated time delay did not change the number of particles predicted to pass the nasal valve, but the predicted deposition sites of these particles changed. With no time delay, approximately 1% of released particles were predicted to deposit on the inferior turbinate and approximately 9% were predicted to deposit on the middle turbinate. With a 0.5-sec delay in the presence of normal inspiratory airflow, 4% to 5% of released particles were predicted to deposit on the inferior turbinate and no particles were predicted to deposit on the middle turbinate (Fig. 6). A time delay of 1 sec produced results equivalent to the cases in which no inspiratory airflow was ever present.

Simulation results for the 1-cm nozzle position were unaffected by refinement of the density of particle release points and were not sensitive to the density of particles released in each spray cone. Left nasal valve penetration fractions of 20- and 50-μm particles released from 1 cm into the nostril in a 1-m/sec, 79° spray were predicted to be 15% and 5% with 30 L/min inspiratory airflow present, respectively.

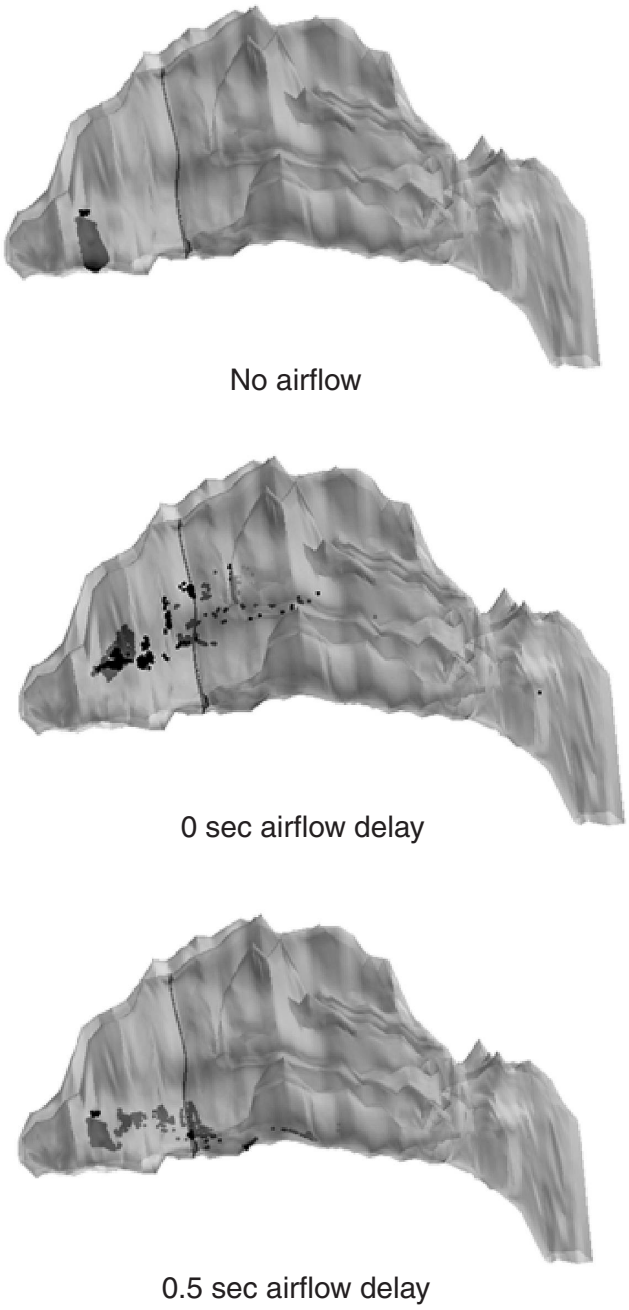

FIG. 6. Effect of a 0.5-sec time delay in the appearance of inspiratory airflow at 15 L/min on the deposition pattern of 20-μm particles released from a nozzle placed 1 cm into the nostril with a velocity of 1 m/sec and a spray angle of 32°.

Confirmation of particle deposition predictions

Simulations predicted that nasal sprays deposit primarily in the anterior part of the nose and that increased particle size decreased nasal valve penetration, in agreement with most experimental studies. Simulations also predicted that better penetration of the nasal valve was achieved at lower initial spray velocities, in agreement with the finding that particles from a nasal nebulizer deposited more posteriorly in the nose than particles from a spray pump.[2]

Simulations of the passive release of particles at the nostril surface did not predict an improvement in nasal valve penetration over low-velocity sprays for 20- and 50-μm particles (Table 3). However, previous simulations with the CFD model used here predicted that the passive release of particles from locations inside the nasal vestibule have greater turbinate deposition than particles passively released at the nostril surface under the same flow conditions.[29] In the nebulizer vs. spray pump study, Suman and colleagues[2] used "a nasal adapter specifically designed to simultaneously administer aerosol into both nostrils without depositing activity on the outside of the nose." Particles emitted from this adapter may have been released inside the nasal vestibule, somewhat distal to the nostril surface. If this were the case, then simulation results were in general agreement with the Suman study findings. However, in that study the nasal nebulizer also produced much smaller particles (approximately 6 μm) than the spray (approximately 79 μm), which would contribute to the difference in deposition patterns.

Simulations predicted a statistically significant effect ($p < 0.001$) of the presence of inspiratory airflow at 15 L/min on the number of particles penetrating the nasal valve, but this effect was considerably smaller at the higher spray velocity of 10 m/sec. This result agreed with the observation that the presence or absence of 10 L/min airflow did not affect regional particle deposition in an experimental study in which spray velocities were higher than 3 m/sec.[6] The highest fractions of 20- and 50-μm particles that were predicted to penetrate the left nasal valve from 1 cm into the nostril did not change appreciably when inspiratory airflow was increased from 15 L/min to 30 L/min. These results are in agreement with the observations that (1) there were no statistically significant differences in nasal distribution patterns of budesonide particles inhaled at 30 or 45 L/min where most particles were larger than 10 μm,[13] and (2) spray deposition was unaffected by gentle or vigorous sniffing in a study where most particles were likely to be larger than 50 μm.[14]

Estimates of nasal deposition efficiency predicted by the CFD model for 6- to 10-μm parti-

cles inhaled at the nostrils at 20 L/min were also compared with experimental measurements of inhaled particles in the same size range at this flow rate. CFD model predictions for the 6- to 10-μm size range agreed well with experimentally measured values (Fig. 7).

Regional particle deposition using nasal spray pumps was previously studied experimentally in a hollow nasal mold constructed from a series of computer-milled plates.[12] Deposition of 50- to 60-μm particles was higher in the turbinate region than in the nasal vestibule for three out of four different spray pumps, and penetration into the nose was generally observed to decrease with increasing spray angle.[12] A fixed nozzle position was used, but no other position information was available. Simulations reported here predicted that the aggregated deposition of 50-μm particles was highest in the nasal vestibule and that there was no statistically significant effect of spray angle on the number of particles penetrating the nasal valve. However, when each release point was examined individually, penetration fractions of 50-μm particles were as high as 21% in the highest aggregate penetration case where particles were released at 1 m/sec with inspiratory airflow present using a spray cone angle of 79°. The highest individual penetration value increased to 33% when the spray cone angle was decreased to 32° (Fig. 8A).

Cheng and colleagues[12] used a polydisperse aerosol, so we examined individual release point penetration for the best 20-μm cases as well. Individual penetration fractions of 20-μm particles were as high as 91% in the highest aggregate penetration case, where particles were released at 1 m/sec with inspiratory airflow present using a spray cone angle of 79°. The highest 20-μm penetration value increased to 100% when the spray cone angle was decreased to 32° (Fig. 8B). If one assumes that a combination of these monodisperse predictions may be used as a crude estimate of actual polydisperse penetration, these results are in agreement with the findings from the Cheng study.[12]

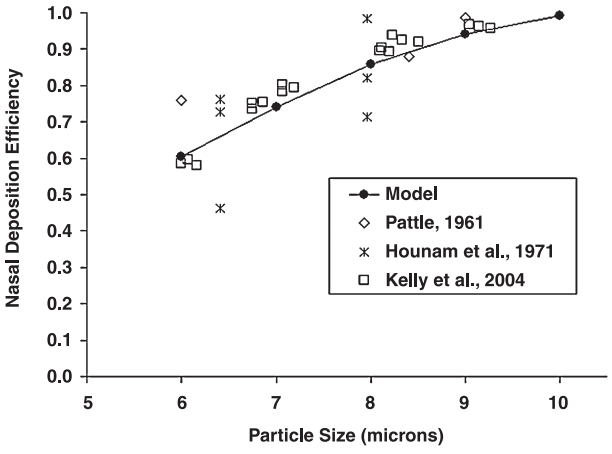

FIG. 7. Comparison of experimentally measured nasal particle deposition efficiency (open symbols)[36,38,40] and simulation results (black circles) for passive release of particles at the nostrils (see Fig. 1B) with 20 L/min steady-state inspiratory airflow present.

DISCUSSION

The CFD model study presented here provided quantitative estimates of the effects that nasal anatomy and different combinations of spray and airflow characteristics may have on nasal valve penetration. This study was undertaken to (1) confirm that the CFD model could capture particle and spray behavior as described in previous experimental studies, (2) suggest reasons for limitations evident in current drug delivery via nasal sprays, and (3) suggest potential ways in which spray penetration could be improved. A CFD approach was used as a comprehensive way to examine nasal drug delivery in an anatomically correct environment.

The estimates obtained here were consistent with measurements obtained experimentally. The ability to compare calculations for multiple combinations of nozzle position and spray characteristics allowed model results to augment existing experimental measurements and provide additional context. Thus, additional interpretations of experimental results were possible, as described above, in the context of particle sizes, spray velocities, inspiratory airflow rates, and spray nozzle positions other than those that had been physically examined.

Major factors limiting the effectiveness of nasal spray devices were identified as (1) physical constraints on the release of particles, such as the small size of areas where particles can be released comfortably and the close proximity of the nasal valve to the tip of the spray device; (2) spray characteristics such as large particle size and high spray velocity; and (3) delayed appearance of inspiratory airflow. Because the physical distance to the nasal valve was only 1 or 2 cm from the point of spray emission (Fig. 3), spray character-

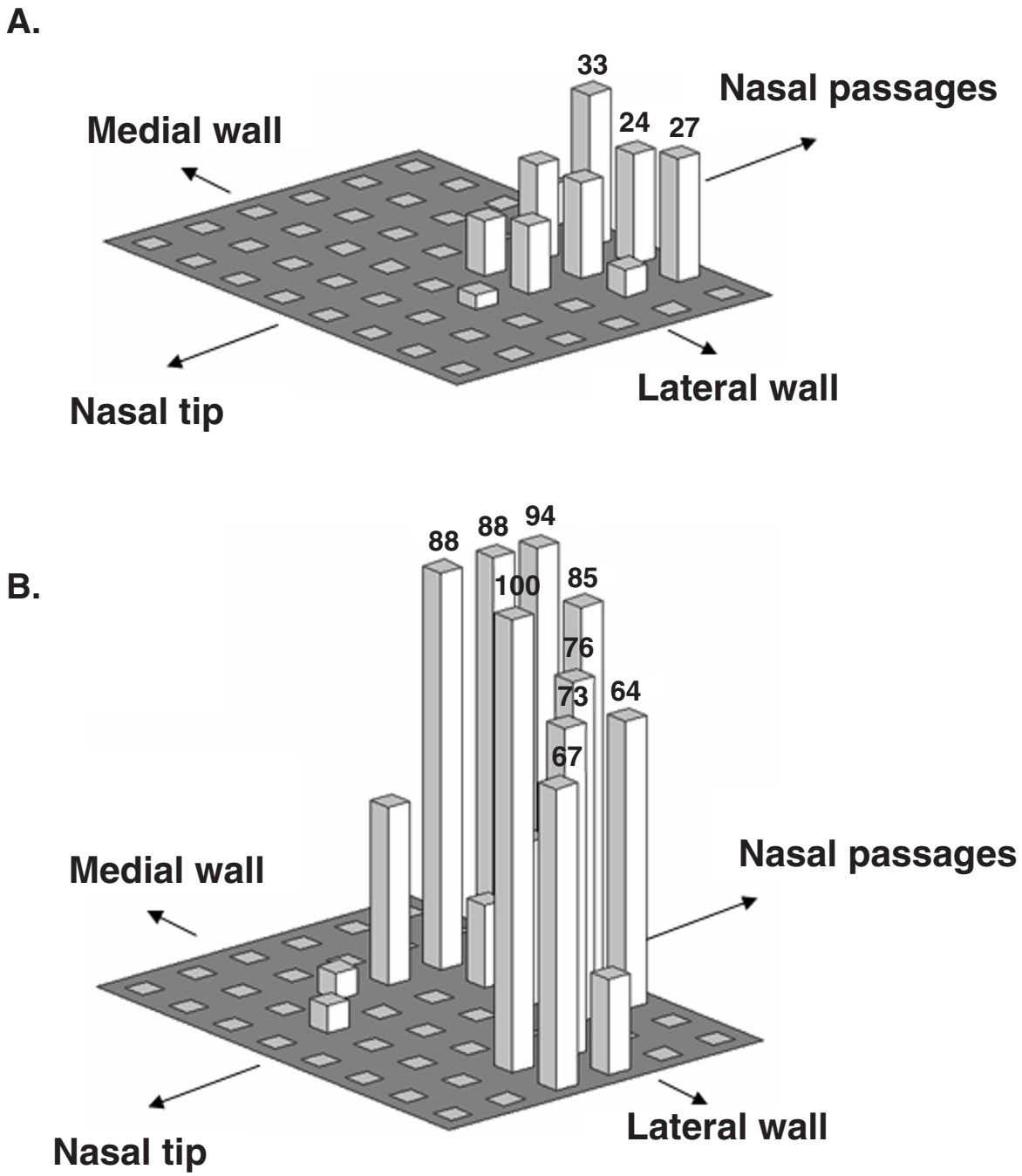

FIG. 8. Nasal valve penetration fractions predicted for each individual release point located 1 cm into the left nasal passage for two sets of parameter values. Steady-state, inspiratory airflow at 15 L/min was present, spray velocity was 1 m/sec, and spray angle was 32° in both cases shown here. (**A**) Plot for the simulated release of 50-μm particles. (**B**) Plot for the simulated release of 20-μm particles. Note that tall bars predict the presence of a "sweet spot" from which a large fraction of released particles penetrate past the nasal valve.

izations measured in open air more than 2 cm from the nozzle tip may be largely irrelevant in the nasal passages. In addition, this study suggested the existence of "sweet spots" for particle release (Fig. 8), which may differ substantially among individual patients.

Among the 48 spray cases simulated, the best nasal valve penetration was predicted when the particle size was 20 μm, spray velocity was 1 m/sec, spray angle was 79°, the spray nozzle was inserted 1 cm into the nose, and gentle inspiratory airflow was present. These results suggested

that nasal valve penetration by nasal sprays could be improved if smaller particles were generated, lower spray velocities were used, particles were released inside the nasal vestibule, and delays between the release of particles and the presence of gentle inspiratory airflow were minimized. These conclusions were based on aggregated results of sprays released at multiple possible points for each nozzle position in order to reduce patient variation in the use of the spray device.

The CFD model also provided new insights into the extent to which the presence and timing of inspiratory airflow could affect nasal spray deposition. For example, the CFD model predicted that with no inspiratory airflow present, almost 50% of 20-μm particles released from 0.5 cm into the nostril at 1 m/sec fell out of the nose through the nostril, with none of the remaining particles penetrating the nasal valve. Under the same spray conditions but with inspiratory airflow present, the CFD model predicted that none of the particles would fall out of the nostril and that 6% of them would able to penetrate past the nasal valve. In another example, a half-second delay in the onset of simulated inspiratory airflow relative to the spray release resulted in a predicted shift of deposition sites from dorsal to ventral locations. Delays longer than 1 sec were predicted to result in the same effects as the case when no airflow had ever been present.

Other information obtained from CFD modeling was the approximate size, shape, and position of the nasal valve as a potential barrier to particle transport. The nasal valve is best described as an area or region in the anterior part of the nose because its size and position can shift with congestion and decongestion (personal communication, Dr. David Wexler, M.D., Fallon Clinic at Worcester Medical Center, Worcester, MA). For the purposes of this study, a single cross-sectional location was identified so that nasal valve penetration could be defined quantitatively, representing a snapshot in time of an individual's nasal passages. The nasal valve cross section used in this study was distal to the anterior margin of the inferior turbinate. Particles predicted to deposit on approximately 0.75 cm of the anterior portion of this turbinate were therefore not included in estimates of the number of particles penetrating the nasal valve. Further study is needed to determine the effects of normal nasal cycling and other congestion on the size, shape, and position of the nasal valve region.

The minimum cross-sectional area (MCA) in the left side of the CFD model was located approximately 3 cm from the left nostril, probably in the vicinity of the pyriform aperture, in agreement with a physiological study that placed the locus of maximal nasal airflow resistance at this region.[17] This location does not compare as well with the distance of 2.3 cm estimated by acoustic rhinometry (AR) in hollow replicas of the CFD model. However, comparisons of distances estimated using AR and MRI or CT scans can be difficult because the axes of sound waves and scans do not generally coincide.[46] MCA predicted by planar cross sections in each side of the CFD model showed reasonable agreement with AR measurements in plastic replicas of the same geometry (Table 2). Total MCA (both sides of the nose added together) was predicted by the CFD model to be 1.36 cm^2 and was in agreement with measurements reported by Millqvist and Bende[47] who used AR to show that MCA in males ranged from 0.40 to 1.00 cm^2 per side, with a mean value of 1.56 cm^2 for total MCA.

The computational mesh underlying the CFD model used here was able to predict total nasal deposition for 20- and 50-μm particles relatively accurately. However, it is possible to skew or grade the distribution of nodes in a CFD mesh toward the walls to improve the accuracy of estimates made at the walls such as regional predicted particle deposition sites. To test the effects of mesh grading on spray simulations, the nasal CFD mesh was truncated just posterior to the nasal valve. More nodes were added to this mesh of the nasal vestibule alone, and the mesh was graded toward the lateral and septal walls. Predicted penetration of the nasal vestibule was unchanged for 50-μm particles and decreased by about 14% for 20-μm particles, suggesting that effects of mesh grading may become more significant as particle size decreases.

With regard to the assumptions underlying the CFD and particle transport models presented here, further study is needed to understand the potential effects of mesh refinements, time-dependent airflow, nonuniform airflow velocity conditions at the nostril, regional heat and humidity conditions, and interindividual differences in nasal anatomy on the nasal spray sensitivity analyses. In the methods used to simulate nasal sprays, the effects of the time dependence of particle size, spray density (temporal evolution of concentration), cone angle, and spray velocity

during spray duration on the sensitivity analyses require more study, as do the potential effects of sprays on inspiratory airflow patterns and interactions of spray particles with each other.

In this study, CFD modeling was used to visualize, quantify, and analyze (1) the role of the nasal valve as a barrier to nasal spray deposition, (2) the very small physical size of likely comfortable particle release areas and their close proximity to the nasal valve, (3) the effects of delaying the presence of inspiratory airflow after particles are released, and (4) the large effects that the presence of inspired airflow as well as smaller particle size and slower spray velocity have on nasal valve penetration. The study suggests that devices that produce large particles at high velocity with no inspiratory airflow present during actuation will have very limited if any nasal valve penetration. Further studies are needed to determine the effects of particle sizes less than 20 μm and of abnormal airway geometry. Along with experimental measurements in hollow molds and human subjects, these predictions contribute to more effective design of drug delivery devices through a better understanding of the interactions between nasal anatomy, sprays, and spray devices and the effects of these interactions on particle transport in the nose.

ACKNOWLEDGMENTS

The authors gratefully acknowledge the contributions and support of R. Conolly, J. Rubis, J. T. Kelly, D. Kalisak, O. Price, J. M. Sheppard, K. Musgrove, B. Bennett, Y. S. Cheng, O. Moss, F. Miller, M. Andersen, A. Georgieva, R. Subramaniam, D. Greenwood, D. Joyner, D. House, and D. Wexler. This work was funded by Bespak Europe Ltd. and the American Chemistry Council.

REFERENCES

1. Bommer, R. 1999. Latest advances in nasal drug delivery technology. Med. Device Technol. 10:22–28.
2. Suman, J.D., B.L. Laube, and R. Dalby. 1999. Comparison of nasal deposition and clearance of aerosol generated by nebulizer and an aqueous spray pump. Pharm. Res. 16:1648–1652.
3. Arora, P., S. Sharma, and S. Garg. 2002. Permeability issues in nasal drug delivery. Drug Discovery Today 7:967–975.
4. Ishikawa, F., M. Murano, M. Hiraishi, T. Yamaguchi, I. Tamai, and A. Tsuji. 2002. Insoluble powder formulation as an effective nasal drug delivery system. Pharmaceut. Res. 19:1097–1104.
5. Hardy, J.G., S.W. Lee, and C.G. Wilson. 1985. Intranasal drug delivery by spray and drops. J. Pharm. Pharmacol. 37:294–297.
6. Hallworth, G.W., and J.M. Padfield. 1986. A comparison of the regional deposition in a model nose of a drug discharged from metered aerosol and metered-pump nasal delivery systems. J. Allergy Clin. Immunol. 77:348–353.
7. Newman, S.P., F. Morén, and S.W. Clarke. 1987. Deposition pattern of nasal sprays in man. Rhinology 26:111–120.
8. Newman, S.P., F. Morén, and S.W. Clarke. 1987. The nasal distribution of metered dose inhalers. J. Laryngol. Otol. 101:127–132.
9. Harris, A.S., E. Svensson, Z.G. Wagner, S. Lethagen, and I.M. Nilsson. 1988. Effect of viscosity on particle size, deposition, and clearance of nasal delivery systems containing desmopressin. J. Pharm. Sci. 77:405–408.
10. Bateman, N.D., A.D. Whymark, N.J. Clifton, and T.J. Woolford. 2002. A study of intranasal distribution of azelastine hydrochloride aqueous nasal spray with different spray techniques. Clin. Otolaryngol. 27: 327–330.
11. Homer, J.J., J. Maughan, and M. Burniston. 2002. A quantitative analysis of the intranasal delivery of topical nasal drugs to the middle meatus: Spray versus drop administration. J. Laryngol. Otol. 116:10–13.
12. Cheng, Y.S., T.D. Holmes, J. Gao, R.A. Guilmette, S. Li, Y. Surakitbanharn, and C. Rowlings. 2001. Characterization of nasal spray pumps and deposition pattern in a replica of the human nasal airway. J. Aerosol Med. 14:267–280.
13. Thorsson, L., S.P. Newman, A. Weisz, E. Trofast, and F. Morén. 1993. Nasal distribution of budesonide inhaled via a powder inhaler. Rhinology 31:7–10.
14. Newman, S.P., K.P. Steed, J.G. Hardy, I.R. Wilding, G. Hooper, and R.A. Sparrow. 1994. The distribution of an intranasal insulin formulation in healthy volunteers: Effect of different administration techniques. J. Pharm. Pharmacol. 46:657–660.
15. Dowley, A.C., and J.J. Homer. 2001. The effect of inferior turbinate hypertrophy on nasal spray distribution to the middle meatus. Clin. Otolaryngol. 26: 488–490.
16. Jones, N. 2001. The nose and paranasal sinuses philology and anatomy. Adv. Drug Deliv. Rev. 51:5–19.
17. Jones, A.S., R.G. Wight, J.C. Stevens, and E. Beckingham. 1988. The nasal valve: A physiological and clinical study. J. Laryngol. Otol. 102:1089–1094.
18. Howard, B.K., and R.J. Rohrich. 2002. Understanding the nasal airway: Principles and practice. Plast. Reconstr. Surg. 109:1128–1144.
19. Hilberg, O., A.C. Jackson, D.L. Swift, and F. Pedersen. 1989. Acoustic rhinometry: Evaluation of nasal cavity geometry by acoustic reflection. J. Appl. Physiol. 66:295–303.

20. Yu, G., Z. Zhang, and R. Lessmann. 1998. Fluid flow and particle diffusion in the human upper respiratory system. Aerosol. Sci. Technol. 28:146–158.
21. Hörschler, I., M. Meinke, and W. Schröder. 2003. Numerical simulation of the flow field in a model of the nasal cavity. Computers Fluids 32:39–45.
22. Keyhani, K., P.W. Scherer, and M.M. Mozell. 1995. Numerical simulation of airflow in the human nasal cavity. J. Biomech. Eng. 117:429–441.
23. Sarangapani, R., and A.S. Wexler. 2000. Modeling particle deposition in extrathoracic airways. Aerosol. Sci. Technol. 32:72–89.
24. Bockholt, U., G. Mlynski, W. Müller, and G. Voss. 2000. Rhinosurgical therapy planning via endonasal airflow simulation. Computer Aided Surg. 5:175–179.
25. Weinhold, I., and G. Mlynski. 2004. Numerical simulation of airflow in the human nose. Eur. Arch. Otorhinolaryngol. 261:452–455.
26. Subramaniam, R.P., R.B. Richardson, K.T. Morgan, R.A. Guilmette, and J.S. Kimbell. 1998. Computational fluid dynamics simulations of inspiratory airflow in the human nose and nasopharynx. Inhal. Toxicol. 10:91–120.
27. Asgharian, B., and S. Anjilvel. 1994. Inertial and gravitational deposition of particles in a square cross section bifurcating airway. Aerosol. Sci. Technol. 20: 177–193.
28. Southall, J.P., H.E. Newell, C.J. Dickens, Y. Al-Suleimani, H. Abduljalil, and A.J. Yule. 2003. Characterization of particle deposition and penetration from current nasal spray devices. Part I—Laboratory characterisation of nasal spray pumps. J. Aerosol. Med. 16:205.
29. Kimbell, J.S., J.D. Schroeter, B. Asgharian, B.A. Wong, R.A. Segal, C.J. Dickens, J.P. Southall, and F.J. Miller. 2004. Optimization of nasal delivery devices using computational models. In R.N. Dalby, P.R. Byron, J. Peary, J.D. Suman, and S.J. Farr, eds. Respiratory Drug Delivery IX, Vol. 1. Healthcare International Publishing, LLC, River Grove, IL, 233–238.
30. Godo, M.N., K.T. Morgan, R.B. Richardson, and J.S. Kimbell. 1995. Reconstruction of complex passageways for simulations of transport phenomena: Development of a graphical user interface for biological applications. Comp. Meth. Prog. Biomed. 47:97–112.
31. Pedley, T.J. 1977. Pulmonary fluid dynamics. Ann. Rev. Fluid Mech. 9:229–274.
32. Asgharian, B., and M.N. Godo. 1997. Transport and deposition of spherical particles and fibers in an improved virtual impactor. Aerosol. Sci. Technol. 27:499–506.
33. Segal, R.A., J.M. Sheppard, and J.S. Kimbell. 2003. Locating the nasal valve with Fieldview. Fluent News 12:15.
34. Deitz, D. 1990. Stereolithography automates prototyping. Mech. Eng. 112:34–39.
35. Kimbell, J.S., and D.D. Greenwood. 1995. Use of stereolithography to construct a three-dimensional physical model of the anterior F344 rat nasal passages. Toxicologist 15:4–5.
36. Kelly, J.T., B. Asgharian, J.S. Kimbell, and B.A. Wong. 2004. Particle deposition in human nasal airway replicas manufactured by different methods. Part I: Inertial regime particles. Aerosol. Sci. Technol. 38:1063–1071.
37. Cheng, Y.S., Yeh, H.C., and Swift, D.L. 1991. Aerosol deposition in human nasal airway for particles 1 nm to 20 μm: A model study. Rad. Prot. Dosim. 38:41–47.
38. Pattle, R.E. 1961. The retention of gases and particles in the human nose. In C.N. Davies, ed. Inhaled Particles and Vapors I. Pergamon Press, Oxford, 302–309.
39. Altshuler, B., E.D. Palmes, and N. Nelson. 1966. Regional aerosol deposition in the human respiratory tract. In C.N. Davies, ed. Inhaled Particles and Vapours II. Pergamon Press, Oxford, 323–335.
40. Hounam, R.F., A. Black, and M. Walsh. 1971. The deposition of aerosol particles in the nasopharyngeal region of the human respiratory tract. J. Aerosol Sci. 2:47–61.
41. Lippmann, M., and R.E. Albert. 1969. The effect of particle size on the regional deposition of inhaled aerosols in the human respiratory tract. Am. Ind. Hyg. Assoc. J. 30:257–275.
42. Lippmann, M. 1970. Deposition and clearance of inhaled particles in the human nose. Ann. Otol. Rhinol. Laryngol. 79:1–10.
43. Heyder, J., and G. Rudolf. 1977. Deposition of aerosol particles in the human nose. In W.H. Walton, ed. Inhaled Particles IV, Part 1. Pergamon Press, Oxford, 107–125.
44. Heyder, J., J. Gebhart, and W. Stahlhofen. 1980. Inhalation of aerosols: Particle deposition and retention. In K. Willeke, ed. Generation of Aerosols and Facilities for Exposure Experiments. Ann Arbor Science, Ann Arbor, MI, 65–103.
45. Snedecor, G.W., and W.G. Cochran. 1967. Statistical Methods, Sixth Edition. The Iowa State University Press, Ames, IA, 325.
46. Hilberg, O., F.T. Jensen, and O.F. Pedersen. 1993. Nasal airway geometry: Comparison between acoustic reflections and magnetic resonance scanning. J. Appl. Physiol. 75:2811–2819.
47. Millqvist, E., and M. Bende. 1998. Reference values for acoustic rhinometry in subjects without nasal symptoms. Am. J. Rhinol. 12:341–343.

Received on November 4, 2005
in final form, September 16, 2006

Reviewed by:
Beth L. Laube, Ph.D.
Chong S. Kim, Ph.D.

Address reprint requests to:
Julia S. Kimbell, Ph.D.
CIIT Centers for Health Research
P.O. Box 12137
Research Triangle Park, NC 27709

E-mail: kimbell@ciit.org

This article has been cited by:

1. X B Chen, H P Lee, V F H Chong, D Y Wang. 2012. Drug delivery in the nasal cavity after functional endoscopic sinus surgery: a computational fluid dynamics study. *The Journal of Laryngology & Otology* 1-8. [CrossRef]
2. K. Inthavong, W. Yang, M. C. Fung, J. Y. Tu. 2012. External and Near-Nozzle Spray Characteristics of a Continuous Spray Atomized from a Nasal Spray Device. *Aerosol Science and Technology* **46**:2, 165-177. [CrossRef]
3. A. Ferré, M. Dres, N. Roche, M. Antignac, M.-H. Becquemin, V. Trosini, L. Vecellio, G. Chantrel, J.-C. Dubus. 2012. Les dispositifs d'inhalation : propriétés, modélisation, réglementation et utilisation en pratique courante. Aérosolstorming du GAT, Paris 2011. *Revue des Maladies Respiratoires* . [CrossRef]
4. Alpár Horváth, Imre Balásházy, Árpád Farkas, Zoltán Sárkány, Werner Hofmann, Aladár Czitrovszky, Erik Dobos. 2011. Quantification of airway deposition of intact and fragmented pollens. *International Journal of Environmental Health Research* 1-14. [CrossRef]
5. Vipra Kundoor, Richard N. Dalby. 2011. Effect of Formulation- and Administration-Related Variables on Deposition Pattern of Nasal Spray Pumps Evaluated Using a Nasal Cast. *Pharmaceutical Research* **28**:8, 1895-1904. [CrossRef]
6. Jeffry D. Schroeter, Guilherme J.M. Garcia, Julia S. Kimbell. 2011. Effects of surface smoothness on inertial particle deposition in human nasal models. *Journal of Aerosol Science* **42**:1, 52-63. [CrossRef]
7. Xiao Bing Chen , Heow Pueh Lee , Vincent Fook Hin Chong , De Yun Wang . 2010. A Computational Fluid Dynamics Model for Drug Delivery in a Nasal Cavity with Inferior Turbinate Hypertrophy. *Journal of Aerosol Medicine and Pulmonary Drug Delivery* **23**:5, 329-338. [Abstract] [Full Text HTML] [Full Text PDF] [Full Text PDF with Links]
8. Xiaofei Liu, William H. Doub, Changning Guo. 2010. Evaluation of droplet velocity and size from nasal spray devices using phase Doppler anemometry (PDA). *International Journal of Pharmaceutics* **388**:1-2, 82-87. [CrossRef]
9. Steven Grunberg, Rebecca A. Clark-Snow, Jim Koeller. 2010. Chemotherapy-induced nausea and vomiting: contemporary approaches to optimal management. *Supportive Care in Cancer* **18**:S1, 1-10. [CrossRef]
10. Revanth Reddy Garlapati, Heow Pueh Lee, Fook Hin Chong, De Yun Wang. 2009. Indicators for the correct usage of intranasal medications: A computational fluid dynamics study. *The Laryngoscope* **119**:10, 1975-1982. [CrossRef]
11. Guilherme J.M. Garcia , Earl W. Tewksbury , Brian A. Wong , Julia S. Kimbell . 2009. Interindividual Variability in Nasal Filtration as a Function of Nasal Cavity Geometry. *Journal of Aerosol Medicine and Pulmonary Drug Delivery* **22**:2, 139-156. [Abstract] [Full Text PDF] [Full Text PDF with Links]
12. Kiao Inthavong, Jiyuan Tu, Goodarz Ahmadi. 2009. Computational Modelling of Gas-Particle Flows with Different Particle Morphology in the Human Nasal Cavity. *The Journal of Computational Multiphase Flows* **1**:1, 57-82. [CrossRef]
13. D DOORLY, D TAYLOR, R SCHROTER. 2008. Mechanics of airflow in the human nasal airways. *Respiratory Physiology & Neurobiology* **163**:1-3, 100-110. [CrossRef]
14. Warren H. Finlay , Andrew R. Martin . 2008. Recent Advances in Predictive Understanding of Respiratory Tract Deposition. *Journal of Aerosol Medicine and Pulmonary Drug Delivery* **21**:2, 189-206. [Abstract] [Full Text PDF] [Full Text PDF with Links]
15. Warren H. Finlay, Andrew R. Martin. 2008. Recent Advances in Predictive Understanding of Respiratory Tract Deposition. *Journal of Aerosol Medicine*, ahead of print080225123426385-18. [CrossRef]
16. Mow Yee Foo , Yung-Sung Cheng , Wei-Chung Su , Maureen D. Donovan . 2007. The Influence of Spray Properties on Intranasal Deposition. *Journal of Aerosol Medicine* **20**:4, 495-508. [Abstract] [Full Text PDF] [Full Text PDF with Links]
17. A FARKAS, I BALASHAZY. 2007. Simulation of the effect of local obstructions and blockage on airflow and aerosol deposition in central human airways. *Journal of Aerosol Science* **38**:8, 865-884. [CrossRef]